

Thermalization of hadrons via Hagedorn states

M. Beitel, K. Gallmeister, and C. Greiner

Institut für Theoretische Physik, Goethe-Universität Frankfurt am Main, Max-von-Laue-Straße 1, 60438 Frankfurt am Main, Germany

(Received 26 February 2014; revised manuscript received 18 July 2014; published 10 October 2014)

Hagedorn states are characterized by being very massive hadron-like resonances and by not being limited to quantum numbers of known hadrons. To generate such a zoo of different Hagedorn states, a covariantly formulated bootstrap equation is solved by ensuring energy conservation and conservation of baryon number B , strangeness S , and electric charge Q . The numerical solution of this equation provides Hagedorn spectra, which also enable us to obtain the decay width for Hagedorn states needed in cascading decay simulations. A single Hagedorn state cascades by various two-body decay channels subsequently into final stable hadrons. All final hadronic observables such as masses, spectral functions, and decay branching ratios for hadronic feed-down are taken from a hadronic transport model. Strikingly, the final energy spectra of resulting hadrons are exponential, showing a thermal-like distribution with the characteristic Hagedorn temperature.

DOI: [10.1103/PhysRevC.90.045203](https://doi.org/10.1103/PhysRevC.90.045203)

PACS number(s): 12.38.Mh, 24.10.Pa, 25.75.Dw, 25.75.Nq

I. INTRODUCTION

In the 1960s physicists were puzzled by the diversity of different hadron species growing with beam energy. Before the emergence of quantum chromodynamics (QCD) as the theory of strong interactions, many ideas arose to explain these findings. Hagedorn [1] proposed to describe the variety of particles found by a common mass spectrum, now better known as Hagedorn spectrum, arising in the framework of a “statistical bootstrap model.” In the infinite mass limit this spectrum is exponentially rising where the slope is determined by the Hagedorn “temperature” T_H . Above this temperature the partition function of a strongly interacting hadronic system with such an exponential growth of states diverges and a new state of matter, the quark gluon plasma (QGP), is assumed to be realized. One of the most challenging problems is to understand how this phase transition exactly occurs and which new properties this new state of matter has. One possible tool to investigate microscopically a phase transition from hadronic to partonic phase is the application and generation of Hagedorn states being created in multi-particle collisions [2–6]. These resonances belong to the continuous part of the Hagedorn spectrum and are allowed to have any mass larger than that of the heaviest known hadron and also any quantum numbers as long as they are compatible with their mass. Such Hagedorn states can alter the occurrence of various phases from hadronic to deconfined partonic matter [7–12].

The abundant appearance of Hagedorn states in the vicinity of T_H helps to explain how chemical equilibrium of hadrons is achieved on timescales significantly smaller than the typical lifetime of a fireball ($t \approx 10 \text{ fm}/c$). In Refs. [4–6], the authors examined chemical equilibration times of (multi)strange (anti)baryons at Relativistic Heavy Ion Collider (RHIC) energies by solving a set of coupled rate equations. It was assumed, that most abundant mesons (pions, kaons) “cluster” to Hagedorn states which in turn decay into (anti)baryons, driving them quickly into equilibrium. For example, the chemical equilibration times of protons, kaons, and lambdas within this approach are of the order of 1–2 fm/ c . The inclusion of Hagedorn states in a hadron resonance gas model provides a

lowering of the speed of sound, c_s , at the phase transition, and is in good agreement with lattice calculations [13–16]. In addition, by comparing calculations with the inclusion of Hagedorn states to calculations without them, a significant lowering of the shear viscosity to entropy ratio, η/s , is observed [13,15,17,18]. The inclusion of Hagedorn states creates a minor dependence of the thermal fit parameters of particle ratios on the Hagedorn temperature, T_H , which is assumed to be equal to T_C [19].

In order to describe the hadronization of jets in e^+e^- annihilation events, different scenarios were developed during the 1970s and 1980s: While the first one assumes independent parton fragmentation [20], the fundamental objects of the second approach are string excitations [21]. Finally, the basic assumption of the latter is that partons tend to cluster in color singlet states from the very beginning of the generated event. These clusters then decay to smaller ones, until some cutoff scale is reached and hadrons are formed [22,23]. An explicit application of the statistical bootstrap model has been used to calculate several properties of particles stemming from decays of hadronic fireballs being created in relativistic heavy ion collisions [24]. In the framework of relativistic quantum molecular dynamics (RQMD) multiparticle collisions and their decays were introduced by the so-called particle clusters a particle system can separate into, provided that separable interactions in the relativistic particle dynamics exist. This clustering is, for example, fulfilled for colored quarks and gluons [25]. Another statistical approach within the microcanonical ensemble addressed the hadronization of quark matter droplets [26]. A further statistical treatment of Hagedorn states was performed in Ref. [27] by forcing detailed balance between creation and decay of Hagedorn states with a simplistic description of the spectrum in the low-mass region. The authors made then the extreme assumption of one single very heavy ($\sim 100 \text{ GeV}$) Hagedorn state subsequently decaying into stable hadrons giving rise to measured particle multiplicities at RHIC and Super Proton Synchrotron (SPS) energies. Terms such as “quark matter droplets,” “clusters,” or “fireballs” may all be identified with possible Hagedorn states, all describing color neutral systems. While none of

them were ever observed directly, the inclusion of such color neutral Hagedorn states helped, for example, to improve the equation of state for many phenomena at hadronization in heavy ion collisions. Thus, Hagedorn states describe the physics close to the border between quark gluon plasma and hadron resonance gas, and hence are a good tool to describe the still not understood hadronization process happening in the phase transition between the two.

The idea is thus to implement Hagedorn states into a transport model, namely ultrarelativistic quantum molecular dynamics (UrQMD) [28], where detailed balance between their production in binary collisions and their decay into two particles only should hold. Before doing so first the branching ratios of Hagedorn states have to be developed, which is the primary aim of this paper. This article is structured as follows. In Sec. II derivation of a covariant bootstrap equation is provided, along with the decay width formula needed to obtain branching ratios of Hagedorn states into various two-particle decay channels. In Sec. III multiplicities of stable hadrons with respect to strong force are shown. Their ratios are then compared to experimental data. In Sec. IV the energy distribution of those decay hadrons is examined; they move freely without further reinteractions, leading to the remarkable result that they all are distributed in energy in a thermal-like manner, exhibiting the same slope which is the Hagedorn temperature T_H , obtained from a fit of the Hagedorn spectrum. Finally in Sec. V a conclusion is drawn showing the opportunities Hagedorn states offer to understand the hadronization process in elementary and also in heavy ion collisions.

II. THEORETICAL FRAMEWORK

The main idea behind the statistical bootstrap model is the postulate stating that fireballs consist of fireballs which in turn consist of fireballs, etc., resulting in a common spectrum with the remarkable feature that it grows exponentially in the infinite mass limit. To put this postulate mathematically one has to count the number of states of a relativistic particle i enclosed in volume V according to [29],

$$dN_i = 2m_i V \frac{d^4 p_i}{(2\pi)^3} \delta(p_i^2 - m_i^2), \quad (1)$$

which is modified to

$$d\tilde{N}_i = 2m_i dm_i \tau_{\vec{C}_i}(m_i) V \frac{d^4 p_i}{(2\pi)^3} \delta(p_i^2 - m_i^2). \quad (2)$$

In Eq. (2), $dm_i \tau_{\vec{C}_i}(m_i)$ is introduced to take into account the mass degeneration. Thus particle i carrying the quantum numbers denoted by $\vec{C}_i = (B_i, S_i, Q_i)$ with four-momentum between p_i and $p_i + dp_i$ might also take on different masses, whose distribution is given by the function $\tau_{\vec{C}_i}$. In the presented work, only the case where two particles make up a Hagedorn state of mass m and volume V is considered. Hence the total number of states of such Hagedorn state made up by two particles is given by a convolution of the constituents' state densities, $d\tilde{n}_i = d^4 \tilde{N}_i / dp_i^4$ for $i = 1, 2$, with the constraint of strict total energy and quantum number conservation. The mass degeneration of the created Hagedorn state is considered

according to Eq. (2) by $\tau_{\vec{C}}$, eventually leading to the bootstrap equation

$$\begin{aligned} \tau_{\vec{C}}(m) &= \frac{R^3}{3\pi m} \sum_{\vec{C}_1, \vec{C}_2} \iint dm_1 dm_2 \tau_{\vec{C}_1}(m_1) m_1 \\ &\quad \times \tau_{\vec{C}_2}(m_2) m_2 p_{cm}(m, m_1, m_2) \delta_{\vec{C}, \vec{C}_1 + \vec{C}_2}, \end{aligned} \quad (3)$$

where p_{cm} denotes the momenta of both constituent particles with masses m_1 and m_2 in the rest frame of made up Hagedorn state with mass m ,

$$p_{cm}(m, m_1, m_2) = \frac{1}{2m} \sqrt{(m^2 - m_1^2 - m_2^2)^2 - 4m_1^2 m_2^2}, \quad (4)$$

as usual. The (spherical) volume V of the Hagedorn state is expressed by its radius, R , which is considered to be constant and set to some physical reasonable values. Contrary to the well known noncovariant bootstrap equation [30,31], the expression here is explicitly covariant. In the generalized solution of (3), the number of constituents can theoretically be more than 2. The reason to consider two constituents case only is because Hagedorn states can and will be implemented in UrQMD as a whole zoo of new particles. In this transport scheme maximally two particles in the incoming channel are allowed because the interaction probability is calculated on the basis of cross sections. On the other hand resonance decays in two hadrons are realized in UrQMD too, making possible an implementation of further ($2 \leftrightarrow 1$) processes, now involving Hagedorn states. For this kind of new processes the principle of detailed balance will strictly hold. The accepted error by the approximation of only two outgoing particles is about 30%, which can be estimated by looking at the Hagedorn state decay probability into n particles, $P(n) = (\ln 2)^{n-1} / (n-1)!$, yielding a probability for the decay into two particles of 69%, into three particles of 24%, etc. [30].

The bootstrap equation (3) in general is a highly nonlinear integral equation of Volterra type which can be solved analytically for some special cases [32,33]. In Sec. III a numerical solution of the bootstrap equation is provided considering the general case containing all hadrons of UrQMD's particle table. The Hagedorn spectra, $\tau_{\vec{C}}(m)$, telling us how many states exist between m and $m + dm$, is needed to formulate the Hagedorn state's creation cross section and its total decay width. The general cross section formula [34] in the center-of-mass frame with creation matrix element $|\mathcal{M}_c|$ reads

$$d\sigma = \frac{(2\pi)^4}{4mp_{cm}} |\mathcal{M}_c|^2 d\Phi_n(p_1 + p_2; p_3, \dots, p_{n+2}). \quad (5)$$

For the production process ($2 \rightarrow 1$) only one particle phase space Φ_1 and the mass degeneration $\tau_{\vec{C}}$ has to be considered, giving

$$\sigma = \frac{\pi |\mathcal{M}_c|^2}{4m^2 p_{cm}} \tau_{\vec{C}}(m). \quad (6)$$

In the same way, the general decay formula [34] with decay matrix element $|\mathcal{M}_d|$ reads

$$d\Gamma = \frac{(2\pi)^4}{2m} |\mathcal{M}_d|^2 d\Phi_n(p; p_1, \dots, p_n). \quad (7)$$

Since only a two-body decay ($1 \rightarrow 2$) is of interest here, calculation of the corresponding two-body phase space Φ_2 is done by taking the mass degeneration for both constituents into account, as was done similarly for the bootstrap equation, resulting in

$$\Gamma_{\vec{C}} = \frac{|\mathcal{M}_d|^2}{8\pi m^2} \sum_{\vec{C}_1, \vec{C}_2} \iint dm_1 dm_2 \tau_{\vec{C}_1}(m_1) \tau_{\vec{C}_2}(m_2) \times p_{cm}(m, m_1, m_2) \delta_{\vec{C}, \vec{C}_1 + \vec{C}_2}. \quad (8)$$

Additionally one has to sum over all pairs of quantum number combinations \vec{C}_1 and \vec{C}_2 which are constrained by Kronecker's δ . It should be reemphasized that, due to the inclusion of the mass degeneration into the decay width as in Eq. (8), the decay scenario of Hagedorn resonances is not phase-space dominated as in, e.g., [29]. On the contrary, the exponentially rising Hagedorn spectra alter drastically the resulting distributions.

In the general formulas for cross section and decay width, the creation and the decay matrix elements $|\mathcal{M}_c|^2$ and $|\mathcal{M}_d|^2$ appear, which for Hagedorn states are at first unknown. By demanding the principle of detailed balance for $2 \leftrightarrow 1$ processes where Hagedorn states involved, $|\mathcal{M}_c|^2 = |\mathcal{M}_d|^2$ holds, and one eventually arrives at

$$\Gamma_{\vec{C}}(m) = \frac{\sigma}{2\pi^2 \tau_{\vec{C}}(m)} \sum_{\vec{C}_1, \vec{C}_2} \iint dm_1 dm_2 \tau_{\vec{C}_1}(m_1) \times \tau_{\vec{C}_2}(m_2) p_{cm}^2(m, m_1, m_2) \delta_{\vec{C}, \vec{C}_1 + \vec{C}_2}. \quad (9)$$

The cross section σ for inelastic scatterings resulting in Hagedorn state production is unfortunately unknown. To make a first, reasonable ansatz for σ the case is considered where two Hagedorn states inelastically collide, producing another Hagedorn state. Since the Hagedorn states are assumed to be spherical with radius R , the fusion cross sections will be considered to be just their geometrical projections, resulting in $\sigma = \pi R^2$. This holds also for processes where two hadrons or a hadron together with a Hagedorn state fuse to a larger Hagedorn state. More sophisticated assumptions about the relevant cross sections are postponed to future studies [35]. Thus Hagedorn state's radius R connects its production with its decay properties via the principle of detailed balance. The partial decay width of a Hagedorn state with mass m and charge vector \vec{C} decaying into two particles with masses m_1, m_2 and charges \vec{C}_1, \vec{C}_2 reads

$$d^2 \Gamma_{\vec{C}, \vec{C}_1, \vec{C}_2}(m, m_1, m_2) = \frac{\sigma}{2\pi^2} p_{cm}^2(m, m_1, m_2) \times \frac{dm_1 \tau_{\vec{C}_1}(m_1) dm_2 \tau_{\vec{C}_2}(m_2)}{\tau_{\vec{C}}(m)} \delta_{\vec{C}, \vec{C}_1 + \vec{C}_2}. \quad (10)$$

The two-body branching ratios \mathcal{B} are just the ratios of partial and total decay widths, Eqs. (10) and (9),

$$d^2 \mathcal{B}_{\vec{C}, \vec{C}_1, \vec{C}_2}(m, m_1, m_2) = \frac{d^2 \Gamma_{\vec{C}, \vec{C}_1, \vec{C}_2}(m, m_1, m_2)}{\Gamma_{\vec{C}}(m)}, \quad (11)$$

needed for calculation of hadronic multiplicities in cascade simulations.

III. SPECTRAL LEVEL DENSITIES AND DECAY WIDTHS

To solve the bootstrap-equation one starts by inserting known hadron spectral functions $\tau_{\vec{C}_i}$ on the right-hand side of Eq. (3), resulting in first Hagedorn states on the left-hand side of this equation. The low-mass inputs are the spectral functions provided by the hadronic table of UrQMD consisting of 55 different baryons and 32 different mesons. In the subsequent steps, these created Hagedorn states serve as constituents in addition to the known sources. In each step, quantum number conservation $\vec{C} = \vec{C}_1 + \vec{C}_2$ is assured. In this way one proceeds by increasing the mass of possible Hagedorn states by steps of $\Delta m = 0.01$ GeV. The computation time increases with mass according to m^8 , since more and more constituent pairs have to be taken into account. Thus the applicability of this approach is limited to the region $m \leq 8$ GeV. The numerical solution of the given bootstrap equation (3) for a meson-like, nonstrange and electrically neutral ($B = S = Q = 0$) Hagedorn spectrum for two different typical radii ($R_1 = 0.8$ fm, $R_2 = 1.0$ fm) is presented in Fig. 1. In the same figure also spectra for baryonic nonstrange and electrically charged states ($B = 1, S = 0, Q = 1$) are shown. All Hagedorn spectra rise exponentially for masses ≥ 1.5 GeV with different slopes for different radii, but for $m < 1.5$ GeV they all include and thus fit the hadronic part of the spectrum. Here lies the major advantage of the present approach, since *ad hoc* assumptions of the kind $\tau(m) = f(m) \exp(m/T_H)$ with most used prefuctions $f(m) = Am^{-b}$ or $f(m) = A(m^2 + m_r^2)^{-b}$ fail to describe the low-mass region of the spectrum. The slopes of the exponential part depend strongly on the size of the Hagedorn state since in a larger one more states can be counted than in a smaller one. The slope parameter is

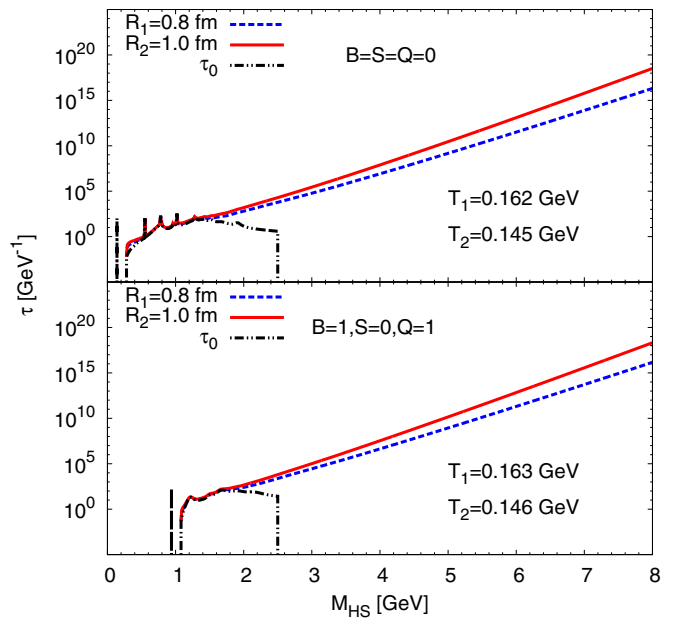


FIG. 1. (Color online) Meson-like ($B = S = Q = 0$) (upper part) and baryonic ($B = 1, S = 0, Q = 1$) (lower part) Hagedorn spectra for two different radii with corresponding (fitted) Hagedorn temperatures. The black line represents the sum of spectral functions of hadrons with the given quantum numbers.

the well known Hagedorn temperature T_H being extracted with the fit function $\tau_{\text{fit}}(m) = Am^{-b} \exp(m/T_H)$, yielding $T_H = 0.145$ GeV for $R = 1.0$ fm and $T_H = 0.162$ GeV for $R = 0.8$ fm. Thus smaller Hagedorn states exhibit a larger Hagedorn temperature depending on the energy density. The Hagedorn temperature range is basically the same for mesonic and baryonic spectra in the presented model, in contrast to [36], where mesonic and baryonic Hagedorn temperatures differ significantly because they were extracted not from the continuous part of the Hagedorn spectrum but solely from its low-mass region. The shown Hagedorn spectra pose the question of why Hagedorn states, especially in the hadronic mass range ($m \leq 2.5$ GeV), have not been observed yet. For example, Hagedorn states like the one at $m = 2$ GeV with quantum numbers $B = Q = 2$ and $S = 0$ are an inevitable consequence of the solution of the bootstrap equation and might be excluded by some more sophisticated approaches. On the other hand there are speculations [36], based on the identification of chiral multiplets, that the particle list of the Particle Data Group [34] is not complete yet. Two major experimental difficulties make Hagedorn states hard to observe: the first one is the large decay width of Hagedorn states [11], and the second, due to the small gaps compared to the widths, is their degree of inseparability for masses beyond the hadronic range. In [36,37] the authors discuss possible missing resonances at low masses such as $m = 1.7$ GeV, or missing strange baryons. In addition, in [38] arguments are given that the large decay width of the Hagedorn states make them hard to observe, as already mentioned.

In Fig. 2 the total decay width of a meson-like, nonstrange and electrically uncharged ($B = S = Q = 0$) Hagedorn state for the same two radii as before is shown. The total decay width of a Hagedorn state consists of three distinct contributions, where the first one considers only hadrons, the second hadrons and Hagedorn states, and the third one only Hagedorn states in the outgoing channel. The peak in the mass range of $M_{HS} = 0-2$ GeV comes mainly from the first contribution, because in this mass range the phase space for pure hadronic decay is largest. The height of the peak depends on the number of hadronic pairs, whose quantum numbers all sum up to the quantum number of the Hagedorn state they are building up, which is large for $B = S = Q = 0$. Another remarkable

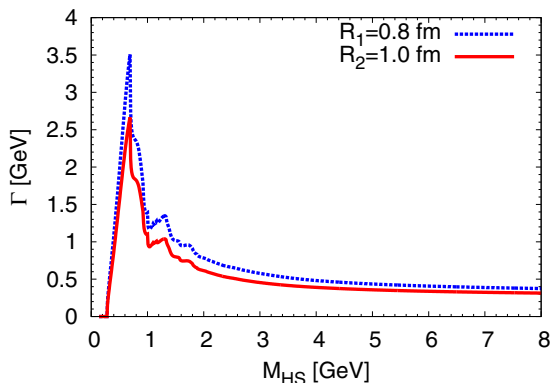


FIG. 2. (Color online) Total decay width of charge neutral Hagedorn state for two different radii.

feature is that for both radii the total decay width tends to a constant value depending only on R . This finding resembles an idea put forward in [11] that the width of a heavy Hagedorn state should depend only on its size.

IV. MULTIPLICITIES AND THERMAL-LIKE ENERGY SPECTRA

Having the numerous branching ratios (11) at hand, one is able to calculate hadronic multiplicities stemming from Hagedorn state decays. Here one starts with some initial (heavy) Hagedorn state, which decays subsequently down until hadrons are left only. Among those also nonstable resonances might appear, which further undergo a hadronic feed-down, leaving one with light and stable hadrons with respect to the strong force, such as pions, kaons, etc.. All hadronic properties used here were taken from the transport model UrQMD.

Calculated multiplicities for some uncharged ($B = S = Q = 0$) initial Hagedorn state are shown in Fig. 3. One observes a linear dependence of all multiplicities on the initial Hagedorn state mass where the magnitude depends on the available phase space for each hadron. Thus, in a decay of a charge neutral Hagedorn state, π^- dominate, which have to be produced in pairs mostly with π^+ since exact charge conservation is enforced. Kaons, especially K^- , are even more strongly suppressed not only because of their larger mass but also due to the fact that they have to conserve both electric charge and strangeness. For the baryons presented the same argument holds, since both have to conserve baryon number B and additionally electric charge Q for proton and strangeness S for Λ . As expected for the multistrange hyperons Ξ^0 and Ω^- the production suppression is even stronger. In

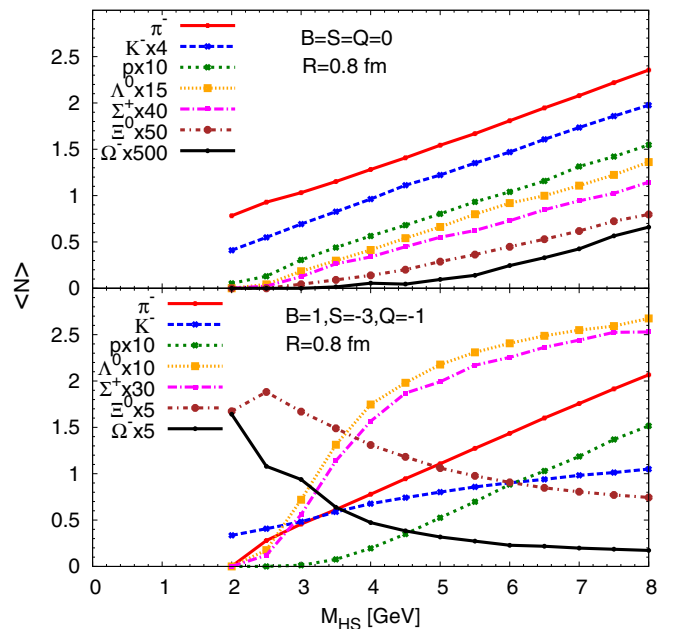


FIG. 3. (Color online) Hadronic multiplicities after a cascade decay of Hagedorn state with radius $R = 0.8$ fm and $B = S = Q = 0$ (upper part) and $B = 1, S = -3, Q = -1$ (lower part) and the following hadronic feed-down.

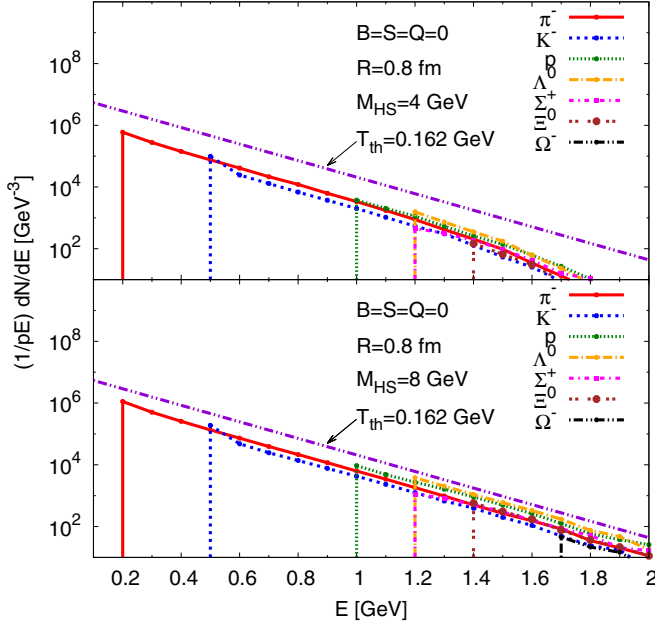


FIG. 4. (Color online) Energy spectra of hadrons stemming from cascade decay of a charge neutral Hagedorn state with radius $R = 0.8$ fm and initial masses $M_{HS} = 4$ GeV and $M_{HS} = 8$ GeV.

the calculations a mean number of strange quarks $\langle s \rangle = 0.548$ at $M_{HS} = 4$ GeV and $\langle s \rangle = 1.232$ at $M_{HS} = 8$ GeV is obtained, confirming the stronger strangeness suppression at low Hagedorn state masses. This has to be contrasted with the results for a baryonic, multistrange, and electrically charged ($B = 1$, $S = -3$, $Q = -1$) Ω^- -like Hagedorn state also shown in Fig. 3. Now the choice of the Hagedorn state's initial quantum numbers is reflected in the preference of baryon production, although they are much heavier than the presented mesons. Especially the abundance of hyperons (Ω^- , Ξ^0) compared to the case discussed before is striking, since the easiest way to conserve the initial quantum numbers is the production of one $\Omega^- \pi^0$ or one $\Xi^0 K^-$ pair, where on the other hand the phase space for all other hadrons with different quantum numbers is suppressed now. Hence exact conservation of quantum numbers always causes a competition between a hadron's phase space and its quantum numbers.

The energy distributions of final hadrons stemming from Hagedorn state decays in these cascading decay simulations are a further intriguing result of this work. They are shown in Fig. 4 for an uncharged ($B = S = Q = 0$) Hagedorn state with initial masses $M_{HS} = 4$ GeV and $M_{HS} = 8$ GeV. The energy distributions for all species presented follow some exponential law with the same slope being independent of the Hagedorn state's initial mass. Thus the energies of these final hadrons have a Boltzmann-like distribution, which in turn means that their distribution obeys a “thermal” state at a temperature of $T_{th} = 0.162$ GeV. This is not established due to multiparticle collisions, because after the decay these final hadrons move freely and do not reinteract with each other again. It is quite remarkable, since this is more or less exactly the Hagedorn temperature (cf. Fig. 1). The Hagedorn temperature T_H was nothing but a slope parameter to fit the

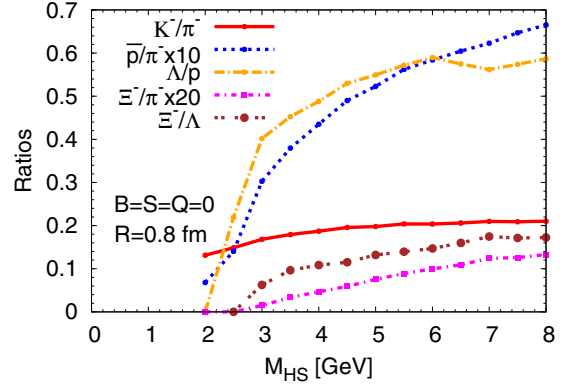


FIG. 5. (Color online) Hadronic ratios stemming from cascade decay of a charge neutral Hagedorn state with radius $R = 0.8$ fm.

exponential part of the Hagedorn spectrum, where on the other hand T_{th} is a slope of Boltzmann-like distribution of the created hadron resonance gas. Starting with a bootstrap formula with no introduction of any notion of temperatures at all resulted in a “thermalized” decay with $T_{th} \simeq T_H$. This has to be contrasted with purely microcanonical considerations, where one assumes that all final states are equiprobable. Due to the derived branching ratios of Eq. (11) plus the final hadronic decays, this is not the case in the present work. Thus, while yielding the same results, namely that the Hagedorn temperature is recovered in the spectra, their origins are different. In the present work, the decay properties are not only phase space dominated, but due to the exponential rising mass degeneration, are modified such that the energy spectra yield the Hagedorn temperature. This result has to be compared with microcanonical analysis of an exponentially growing mass spectrum, where the occurrence of thermally and chemically equilibrated hadron gas at the Hagedorn temperature in contact with a Hagedorn thermostat [7] has been demonstrated.

In Fig. 5 various ratios of the most interesting stable hadrons stemming from a decay of an uncharged ($B = S = Q = 0$) Hagedorn state with $R = 0.8$ fm are presented. Numerical values for the multiplicity ratios for Hagedorn state masses of 4 and 8 GeV are listed in Table I and compared to experimental results for p - p and Pb-Pb collisions at midrapidity, both

TABLE I. Comparison of particle multiplicity ratios from theory vs p - p at $\sqrt{s_{NN}} = 0.9$ TeV [39] and Pb-Pb at $\sqrt{s_{NN}} = 2.76$ TeV [40–42], both from ALICE at LHC. Calculated values are listed for Hagedorn state masses of 4 GeV and 8 GeV. Numbers in brackets denote the error in the last digits of the multiplicity ratios.

	p-p	Pb-Pb	4 GeV	8 GeV
K^-/π^-	0.123(14)	0.149(16)	0.187	0.210
\bar{p}/π^-	0.053(6)	0.045(5)	0.043	0.066
Λ/π^-	0.032(4)	0.036(5)	0.021	0.038
Λ/\bar{p}	0.608(88)	0.78(12)	0.494	0.579
Ξ^-/π^-	0.003(1)	0.0050(6)	0.0023	0.0066
$\Omega^-/\pi^- \cdot 10^{-3}$	—	0.87(17)	0.086	0.560

measured by the ALICE Collaboration at the Large Hadron Collider (LHC).

The theoretical multiplicity ratios lie rather close to ones measured by ALICE, except for the very rare multi-strange baryon Ω^- . However, it has to be made clear that the decay of Hagedorn states alone is never assumed to describe the experimental data in heavy ion collisions. On the contrary, Hagedorn state branching ratios in (11) appear physically reasonable and reliable, enabling one to implement these Hagedorn states into a full dynamical picture of UrQMD. Results of these investigations will be presented in upcoming papers [35], which are beyond the scope of this article.

V. CONCLUSIONS

In the context of heavy ion collisions Hagedorn states have to be considered as a phenomenological tool to describe the phase transition from the quark gluon plasma to the hadron resonance gas. This phase transition is believed to occur around the critical temperature T_c , which in our understanding equals the Hagedorn temperature T_H , where Hagedorn states appear most abundantly. At this stage of phase transition they serve as “intermediate” states which decay directly or via a decay chain into final known hadrons. Also in smaller systems like e^+e^- or p - p lighter color neutral blobs or clusters may be created which solely decay [22,23]. For such small systems one employed thermal descriptions with exact conservation of strangeness [43] or incorporating a strangeness suppression factor γ_s [44] where the conditions for their applicability were investigated in [45,46]. On the other hand, in relativistic heavy ion collisions larger objects may be generated which then also

interact and are decaying and regenerated. This may lead to a faster equilibration close to the phase transition [4,6] and might explain the success of the statistical model [47,48]. The statistical model has also been employed for much smaller systems in elementary collisions [45,46]. One of the defined goals of the PANDA collaboration at the Facility for Antiproton and Ion Research (FAIR, Darmstadt) is the search for new exotic states [49].

Summarizing, such a finding gives new insight into the microscopic and thermal-like hadronization in ultrarelativistic e^+e^- (see, e.g., [44]), hadron-hadron, and especially heavy ion collisions: An implementation of the presented Hagedorn state decays in addition to their production mechanisms into the transport approach UrQMD offers a new venue for allowing hadronic multiparticle collisions in a consistent scheme, which is important in the vicinity of the deconfinement transition. Understanding faster thermalization and chemical equilibration, and also microscopic transport properties, can be thoroughly investigated in the future [35].

ACKNOWLEDGMENTS

The authors acknowledge discussions with R. Bellwied, K. Bugaev, L. Moretto, J. Noronha-Hostler, R. Stock and H. Stöcker. This work was supported by the Bundesministerium für Bildung und Forschung (BMBF), HGS-HIRE and the Helmholtz International Center for FAIR within the framework of the LOEWE program launched by the State of Hesse. Numerical computations have been performed at the Center for Scientific Computing (CSC).

-
- [1] R. Hagedorn, *Nuovo Cimento Suppl.* **3**, 147 (1965).
 - [2] C. Greiner and S. Leupold, *J. Phys. G* **27**, L95 (2001).
 - [3] C. Greiner, P. Koch-Steinheimer, F. M. Liu, I. A. Shovkovy, and H. Stoecker, *J. Phys. G* **31**, S725 (2005).
 - [4] J. Noronha-Hostler, C. Greiner, and I. A. Shovkovy, *Phys. Rev. Lett.* **100**, 252301 (2008).
 - [5] J. Noronha-Hostler, C. Greiner, and I. Shovkovy, *J. Phys. G* **37**, 094017 (2010).
 - [6] J. Noronha-Hostler, M. Beitel, C. Greiner, and I. Shovkovy, *Phys. Rev. C* **81**, 054909 (2010).
 - [7] L. Moretto, K. Bugaev, J. Elliott, and L. Phair, *Europhys. Lett.* **76**, 402 (2006).
 - [8] I. Zakout, C. Greiner, and J. Schaffner-Bielich, *Nucl. Phys. A* **781**, 150 (2007).
 - [9] I. Zakout and C. Greiner, *Phys. Rev. C* **78**, 034916 (2008).
 - [10] L. Ferroni and V. Koch, *Phys. Rev. C* **79**, 034905 (2009).
 - [11] K. A. Bugaev, V. K. Petrov, and G. M. Zinovjev, *Phys. Rev. C* **79**, 054913 (2009).
 - [12] A. I. Ivanytskyi, K. A. Bugaev, A. S. Sorin, and G. M. Zinovjev, *Phys. Rev. E* **86**, 061107 (2012).
 - [13] J. Noronha-Hostler, J. Noronha, and C. Greiner, *Phys. Rev. Lett.* **103**, 172302 (2009).
 - [14] A. Majumder and B. Muller, *Phys. Rev. Lett.* **105**, 252002 (2010).
 - [15] J. Noronha-Hostler, J. Noronha, and C. Greiner, *Phys. Rev. C* **86**, 024913 (2012).
 - [16] A. Jakovac, *Phys. Rev. D* **88**, 065012 (2013).
 - [17] M. I. Gorenstein, M. Hauer, and O. N. Moroz, *Phys. Rev. C* **77**, 024911 (2008).
 - [18] K. Itakura, O. Morimatsu, and H. Otomo, *J. Phys. G* **35**, 104149 (2008).
 - [19] J. Noronha-Hostler, H. Ahmad, J. Noronha, and C. Greiner, *Phys. Rev. C* **82**, 024913 (2010).
 - [20] R. Field and R. Feynman, *Nucl. Phys. B* **136**, 1 (1978).
 - [21] B. Andersson, G. Gustafson, G. Ingelman, and T. Sjostrand, *Phys. Rept.* **97**, 31 (1983).
 - [22] B. Webber, *Nucl. Phys. B* **238**, 492 (1984).
 - [23] G. Marchesini, B. Webber, G. Abbiendi, I. Knowles, M. Seymour *et al.*, *Comput. Phys. Commun.* **67**, 465 (1992).
 - [24] R. Hagedorn and J. Rafelski, *Phys. Lett. B* **97**, 136 (1980).
 - [25] H. Sorge, H. Stoecker, and W. Greiner, *Ann. Phys. (N.Y.)* **192**, 266 (1989).
 - [26] K. Werner and J. Aichelin, *Phys. Rev. C* **52**, 1584 (1995).
 - [27] S. Pal and P. Danielewicz, *Phys. Lett. B* **627**, 55 (2005).
 - [28] S. Bass, M. Belkacem, M. Bleicher, M. Brandstetter, L. Bravina *et al.*, *Prog. Part. Nucl. Phys.* **41**, 255 (1998).
 - [29] E. Byckling and K. Kajantie, *Particle Kinematics* (John Wiley & Sons, London, 1973).
 - [30] S. C. Frautschi, *Phys. Rev. D* **3**, 2821 (1971).

- [31] C. Hamer and S. C. Frautschi, *Phys. Rev. D* **4**, 2125 (1971).
- [32] J. Yellin, *Nucl. Phys. B* **52**, 583 (1973).
- [33] R. Hagedorn and I. Montvay, *Nucl. Phys. B* **59**, 45 (1973).
- [34] J. Beringer *et al.* (Particle Data Group), *Phys. Rev. D* **86**, 010001 (2012).
- [35] M. Beitel, K. Gallmeister, and C. Greiner (unpublished).
- [36] W. Broniowski, W. Florkowski, and L. Y. Glozman, *Phys. Rev. D* **70**, 117503 (2004).
- [37] A. Bazavov, H.-T. Ding, P. Hegde, O. Kaczmarek, F. Karsch, *et al.*, *Phys. Rev. Lett.* **113**, 072001 (2014).
- [38] K. Bugaev, V. Petrov, and G. Zinovjev, *Europhys. Lett.* **85**, 22002 (2009).
- [39] K. Aamodt *et al.* (ALICE Collaboration), *Eur. Phys. J. C* **71**, 1594 (2011).
- [40] B. Abelev *et al.* (ALICE Collaboration), *Phys. Rev. C* **88**, 044910 (2013).
- [41] B. B. Abelev *et al.* (ALICE Collaboration), *Phys. Rev. Lett.* **111**, 222301 (2013).
- [42] B. B. Abelev *et al.* (ALICE Collaboration), *Phys. Lett. B* **728**, 216 (2014).
- [43] J. Cleymans, K. Redlich, and E. Suhonen, *Z. Phys. C* **51**, 137 (1991).
- [44] F. Becattini, *Z. Phys. C* **69**, 485 (1996).
- [45] J. Hormuzdiar, S. D. Hsu, and G. Mahlon, *Int. J. Mod. Phys. E* **12**, 649 (2003).
- [46] D. H. Rischke, *Nucl. Phys. A* **698**, 153 (2002).
- [47] P. Braun-Munzinger, J. Stachel, J. Wessels, and N. Xu, *Phys. Lett. B* **365**, 1 (1996).
- [48] P. Braun-Munzinger, D. Magestro, K. Redlich, and J. Stachel, *Phys. Lett. B* **518**, 41 (2001).
- [49] E. Fioravanti ($\bar{\text{P}}$ ANDA Collaboration), *J. Phys. Conf. Ser.* **503**, 012030 (2014).